This is a preprint draft. The published article can be found at: http://doi.org/10.1002/fam.3116.

Please cite this paper as:
Karaki, G., Naser, M.Z. (2022). An approach for developing probabilistic models for temperature-dependent properties of construction materials from fire tests and small data. *Fire and Materials*. http://doi.org/10.1002/fam.3116.

An approach for developing probabilistic models for temperature-dependent properties of construction materials from fire tests and small data

G. Karaki[1*], M.Z. Naser[2]

[1]Assistant Professor, Department of Civil and Environmental Engineering, Birzeit University, Birzeit, Palestine
E-mail: gkaraki@birzeit.edu

[2]Assistant Professor, School of Civil & Environmental Engineering and Earth Sciences (SCEEES), Clemson University, USA
[3]AI Research Institute for Science and Engineering (AIRISE), Clemson University, Clemson, SC, USA
E-mail: mznaser@clemson.edu, Website: www.mznaser.com
*Corresponding author

Abstract

Probabilistic approaches provide a more realistic look into assessing structures under fire conditions and overcome some limitations observed in the more traditional (deterministic) approaches. These approaches have also been introduced to the fire engineering domain, e.g., fire probabilistic risk analysis and probabilistic structural fire engineering. In order to perform probabilistic-based analysis, temperature-dependent probabilistic models for material properties are needed. This paper presents a methodology to develop temperature-dependent probabilistic models for the thermal and mechanical properties for commonly used construction materials, including normal-strength, high-strength, and high-performance concrete and mild, high-strength, and cold-formed steels. The presented approach analyzes a comprehensive list of surveyed experimental data at different temperature groups, tests the goodness of fit for a number of distributions, and derives a continuous function to quantify temperature-dependent parameters of the distribution. In addition, the newly derived models are also compared against those adopted by fire codes, and standards and others derived using machine learning. The newly developed models will complement existing efforts to facilitate probabilistic performance-based structural fire engineering.

Keywords: fire, probabilistic models, material properties, approach

1. Introduction

The structural assessment for buildings exposed to fire requires knowledge of fire characteristics, building layout, loading conditions, and properties of present construction materials [1]. While fire resistance evaluation primarily favors deterministic approaches to assess fire response of structural systems, temperature-dependent material models for properties of the different construction materials are not always available with high confidence. Codes, standards and reports, i.e., ASCE manual on structural fire protection [2], ACI guide [3], Eurocode 2, 2004 [4] and Eurocode 3, 2005 [5], Harmathy [6], Bennetts [7], Schneider [8], and Anderberg [9], documented, surveyed, and discussed the mechanical and thermal properties of the different building materials. Models for the thermal and mechanical properties of some building materials at elevated temperatures can be found in ASCE, 1992 [10], Eurocode 2, 2004 [4], and Eurocode 3, 2005 [5]. In general, these are developed as a function of temperature in the temperature range of (0 – 1000 ^{o}C). It should be noted that most of the codes and standards relationships for the thermal and mechanical properties at elevated temperatures present the averages of surveyed observations [3]. Furthermore, the material properties at elevated temperatures data are based on steady-state and transient state tests and sometimes a combination of both [11]. Most codes and standards, e.g., Eurocode 2, 2004 [4], offer no distinction between HSC and NSC in their fire design provisions and no specific information on whether the design rules were specified for concrete under service load [11]. Thus, engineers often utilize such material models adopted in fire codes and standards, which are developed using material tests undertaken in the late 1980s-2000s and belonged to varying testing procedures and different geographical regions [12]. Practically speaking, such models may prove outdated and could potentially and adversely affect the reliability of the fire structural capacity assessment.

The open literature offers models for temperature-dependent properties of assumed typical construction materials, such as normal-strength concrete and steel [13,14]. A limited number of published works (e.g. [12,15–19] proposed temperature-dependent material models for modern materials used in the construction industry, e.g., high-strength concrete and high-strength steel. Much of the reviewed models were arrived at via small-scale material tests – often on a limited number of specimens and confined into a particular testing methodology [20].

More recently, probabilistic approaches have been introduced to fire engineering, e.g., probabilistic fire risk analysis (PRA) and more extended probabilistic structural fire engineering (PSFE) [21]. The probabilistic analysis provides a more realistic look into the assessment of structures under fire conditions, and it aims to overcome some of the limitations observed in the more traditional (deterministic) approaches by including uncertainties stemming from the simplifications and assumptions used in systems analysis and design processes. Van Coile et al. [22] provide discussions and clarifications related to probabilistic risk assessment (PRA), which is usually used as a tool for performance-based design in fire safety engineering. Furthermore, the paper presents a hierarchy of the different acceptance concepts. Shrivastava et al. [23] adapted the Performance-Based Earthquake Engineering framework for application to structural fire engineering, which required identifying potential fire severity measures. The developed framework facilitates the evaluation of the damage probability or failure probability of a structure due to a probable fire hazard within the framework of PSFE. Gernay et al. [24] present frameworks for PSFE and development of fragility curves which are essential to evaluate the probabilistic vulnerability of structural members and systems exposed to fire scenarios. The techniques developed in this paper help establish reliability levels used to assess the resilience for the different fire scenarios. The probabilistic modeling and analysis frameworks and techniques require the inclusion of uncertainties. Such uncertainties can broadly be grouped under two categories: model and parameter (variable) uncertainties.

Please cite this paper as:
Karaki, G., Naser, M.Z. (2022). An approach for developing probabilistic models for temperature-dependent properties of construction materials from fire tests and small data. *Fire and Materials*. http://doi.org/10.1002/fam.3116.

Model uncertainty is related to the mathematical model of the engineering problem, while parameter uncertainty is linked to uncertainty in variable estimates (which is tied to the amount and quality of collected information for the input variables [25]. Building on the motivation of this work, this study aims to examine the uncertainty in material models pertaining to material properties (i.e., falls within the category of variable uncertainty). Therefore, to include their uncertainties in assessing the structural capacities of fire-damaged buildings, there is a need to derive temperature-dependent probabilistic models for temperature-dependent material properties.

Some research works have explored the notion of uncertainty within the variables defining thermal and mechanical properties of typical construction materials (i.e., normal-strength concrete and mild steel) and thermal properties of insulating materials, e.g. [24,26–28]. However, a smaller number of research works derived temperature-dependent probabilistic models for the construction material properties. In one notable study, Khorasani et al. (2015) [29] developed probabilistic models for the mechanical properties of mild steel and the thermal properties for insulating materials using a Bayesian statistical approach. The mechanical properties of mild steel and normal-strength concrete were also examined by Qureshi et al. (2020) [30]. These researchers developed probabilistic temperature-dependent material models using fitted continuous probability distribution functions. Furthermore, probabilistic models for the thermal properties for normal-strength concrete were developed by Jovanović et al. (2020) [31] and Karaki et al. (2021) [32].

In support of recent calls to adopt probabilistic approaches, this paper presents a methodology to develop temperature-dependent probabilistic models for material properties. In addition, this paper also provides probabilistic models for the properties of a variety of cementitious and metallic construction materials. These models were developed using a comprehensive list of surveyed experimental data for the thermal and mechanical properties of Normal-Strength Concrete (NSC), High-Strength Concrete (HSC), High-Performance Concrete (HPC), Mild Steel (MS), High-Strength Steel (HSS), and Cold-Formed Steel (CFS). The newly developed models will complement existing efforts to facilitate probabilistic performance-based structural fire engineering.

2. Data collection of temperature-dependent material properties

The properties of construction materials are usually tested using small-scale specimens, i.e., concrete cubes/cylinders of metal coupons. The tested specimens are heated uniformly to a specified temperature using furnaces or electric ovens and loaded until failure. The majority of the data surveyed were obtained from steady-state and transient tests[1] and found in the following research works [33–71].

[1] Noting that fire is a complex phenomenon that may not follow a pure steady state or transient nature, we opt to combine steady state and transient tests into one database. Future works can still apply our methodology toward exploring the influence of testing procedure on the developed material models. Additional details on our approach can be found in the Methodology section.

This is a preprint draft. The published article can be found at: http://doi.org/10.1002/fam.3116.

Please cite this paper as:
Karaki, G., Naser, M.Z. (2022). An approach for developing probabilistic models for temperature-dependent properties of construction materials from fire tests and small data. *Fire and Materials*. http://doi.org/10.1002/fam.3116.

After examining the different publications on temperature-dependent material properties, it was observed that researchers were using different specimen sizes, boundary conditions, specified heating and cooling rates, and loading conditions. This reflects the lack of an international and well-established standardized procedure to test cementitious and metallic specimens to evaluate the temperature-dependent material properties [12,20,72,73]. A review of the experimental data on the behavior of construction materials can be found in multiple publications, e.g. [12,18,19,74–77].

3. Methodology for Development of Probabilistic Models:

Probabilistic material models are continuous models that derive temperature-dependent functions for a set of parameters defining the fitted probability distribution functions. The methodology comprises the following steps.

Survey and collect experimental data: for most of the material properties examined, a minimum of eight tests were collected and used to derive the probabilistic material models. Every test surveyed the related material property at target temperature points (i.e., 25, 100, 200… 1000°C). All selected tests were mainly conducted within the last two decades and naturally varied by origin institutes and laboratories. The aforenoted “selection criteria” for the collected tests ensured that data used in deriving the probabilistic models represent current advances in construction material sciences, and reflect materials available in the market. This will yield relevant probabilistic models with a wide range of applications.

Choose the family of distribution functions: the compiled data for mechanical and thermal properties contains property values for target (specific) temperatures in the range of 25, 100, 200, 300 … 1000ºC. Every data set was fitted to basic distribution functions that are: 1) commonly used, and 2) require a small number of parameters (with a maximum of two depending on the distribution function). Six distribution functions were tested for every property, namely: Normal, Lognormal, Logistic, Loglogistic, Birnbaum-Saunders, Weibull distributions.

Check goodness of fit: generally speaking, the sample size of the available data sets is small (as noted in parallel works [12,18,19]); therefore, the goodness of fit would rely on a multi-step assessment procedure where the available statistical tools were combined with the modeler’s judgment on available data. From this perspective, the best model is the one that delivers an acceptable description of the data while using a minimum number of parameters to yield a compact representation. The most popular penalized-likelihood criteria for model selection are the Akaike Information Criterion (AIC) and Bayesian Information Criterion (BIC), [78]. Despite the differences in their assumptions and theoretical background, their difference in practice is the size of the penalty on free parameters. BIC penalizes model complexity more than AIC, which means BIC and AIC disagree when AIC chooses a more complex model to describe the data. Furthermore, BIC is more consistent than AIC when data size is large [78,79]. As mentioned in the previous step, basic models with equal complexity were selected as candidate models. Building on the fact that the sizes of the surveyed data are small, the AIC criteria were chosen to check the goodness of fit for the candidate models. AIC estimators indicate the model with the lowest expected information loss. Furthermore, to account for the effect of small data sizes on likelihood estimation, a corrected Akaike estimator (AIC_c) is often used, which adds the term $\left(\frac{2V(V+1)}{(n-V-1)}\right)$ to penalize the small data size. AIC_c estimator is expressed in Eq. (1),

$$AIC_c = -2\log L + 2V + \frac{2V(V+1)}{(n-V-1)} \tag{1}$$

where L is the maximum likelihood for the candidate model, V is the number of the model's parameters, and n is the number of samples.

The model with a smaller value of AIC_c is considered the one with the lowest information loss. However, AIC_c values can be transformed to conditional probabilities for each model; these probabilities are referred to as Akaike weights [79], Eq. (2).

$$w_i(AIC_c) = \frac{\exp\left\{-\frac{1}{2}\Delta_i(AIC_c)\right\}}{\sum_{k=1}^{K} \exp\left\{-\frac{1}{2}\Delta_k(AIC_c)\right\}} \tag{2}$$

where $\Delta_i(AIC_c)$ is the difference between the AIC_c of the i^{th} model and the minimum value of AIC_c for all candidate models, and K is the number of all candidate models. Akaike weight (w_i) represents the probability that the i^{th} model has the lowest information loss given the data, and the other candidate models examined [79]. The models with high values of Akaike weights are considered the best candidates to represent the data sets. The weights were used to select a subset from all model candidates for further examination.

Develop continuous models for the parameters of selected probability distribution functions: Regression models are then used to derive a relation for the parameters defining the selected distribution functions as a continuous function of temperature. Scatter plots of distribution parameters were the initial tool to check the quality of the regression model and were used to avoid the overfitting of the data (variance). Furthermore, the coefficient of determination R^2 was used to check the approximation quality and prevent underfitting the data (bias), Eq. (3). Other supplementary metrics (such as R) can also be used as per the modeler's preference.

$$R^2 = 1 - \frac{SS_{res}}{SS_{tot}} \tag{3}$$

$$SS_{res} = \sum_{i=1}^{n} (y_i - f_i)^2 \tag{3.a}$$

$$SS_{tot} = \sum_{i=1}^{n} (y_i - \bar{y})^2 \tag{3.b}$$

where y_i is the data point, $\bar{y}$ is the mean value of data points, and f_i is the fitted data point.

Generally, and given their simplicity, polynomial functions with first, second, and third orders were tested as candidates for the regression model. Higher-order polynomials were avoided as overfitting was noticed. Furthermore, a general flattening effect was apparent in the scatter plots of the data points for yield strength and modulus of elasticity of the steel, which polynomial functions could not model. Therefore, an exponential function was introduced for their models to even the peaks of the polynomial function.

Document the probabilistic model: A subset of the candidates to define the probabilistic models were selected following the goodness of fit for the distribution function and the regression models for distribution parameters. A final check for conditions on the values of the material properties (when required) was performed. For example, the data available for concrete strength is normalized by the strength at ambient temperature; thus, experimental data were positive values. The selected model needed to produce positive values. Furthermore, if the data sets prove to be too small to indicate the best fit for the candidate models, then a normal or lognormal distributions were chosen based on data points. The candidate from the subset with the best-fit estimators with realistic values for the material property was selected, visualized, and documented.

4. Developed Models

The methodology is illustrated in detail for the compressive strength of normal-strength concrete and modulus of elasticity of mild steel as dedicated examples. Furthermore, the developed models for the thermal and mechanical material properties for Normal-Strength Concrete (NSC), High-Strength Concrete (HSC), High-Performance Concrete (HPC), Mild Steel (MS), High-Strength Steel (HSS), and Cold-Formed Steel (CFS) are presented in the following section.

4.1 Implementation

The data points for the material property were fitted at every temperature point to each one of the following distributions; Normal, Lognormal, Logistic, Loglogistic, Birnbaum-Saunders, and Weibull. The *AICc* estimator of prediction error was calculated at every temperature point. An overall AIC_c measure for the candidate model was then calculated as the sum of AIC_c estimators at the examined temperatures, for which the Akaike weight was calculated. Akaike weight presents the conditional probability that the candidate model describes the data with the lowest data loss. Table 1 shows the results for fitting the data for the compressive strength of normal-strength concrete. A subset from candidate models was chosen based on the values of Akaike weights. Every subset contained two to three candidates' models that had the relatively highest Akaike weights, with an assumed 0.2 weight as a lower limit. Accordingly, from the six distribution functions, a subset of three distributions, i.e., Lognormal, Birnbaum-Saunders, and Loglogistic distributions, were selected to be further examined in the following step: modeling the distribution functions and regenerating the data points using the regression models. The model with the highest weight was tested first. If the regression models for the distribution variables were of relatively good quality and presented the original data, then this distribution and the regression models of its parameters were accepted and documented. Otherwise, the second-best distribution was tested, and so forth.

Table 1. The *AICc* estimators and Akaike weights for the fitted distribution functions of compressive strength for normal-strength concrete

Distribution	AIC_i	w_i	Distribution	AIC_i	w_i
Normal	-207.91	0.12	Loglogistic	-208.89	**0.20**
Lognormal	-209.83	**0.31**	Weibull	-205.18	0.03
Logistic	-206.28	0.05	Birnbaum-Saunders	-209.66	**0.29**

Following the above explanation, the lognormal distribution was examined first for the compressive strength of normal-strength concrete. This distribution is defined using two parameters; mean value (μ) and standard deviation (σ). The distribution parameters-temperature relationship was modeled using different degrees of polynomial functions. The coefficient of determination and scatter plots were used to assess the quality of the developed regression models. Eq. (4) describes the μ and σ values as a function of temperature.

$$\mu = 0.0262 - 0.5103 \cdot T_{std} + 1.3704 \cdot T_{std}^2 - 2.7088 \cdot T_{std}^3 \quad (4a)$$

$$\sigma = 0.0650 - 0.1172 \cdot T_{std} + 0.6207 \cdot T_{std}^2 \quad (4b)$$

T_{std} is the standardized temperature, i.e. $T_{std} = (T_i - T_{min})/(T_{max} - T_{min})$, where T_i is the examined temperature point, T_{min} is the minimum temperature in data set, and T_{max} is the maximum temperature in the data set. By using the standardized temperatures', the determination of regression coefficients was more stable. The coefficient of determination for the regression model of μ is 0.99 and of σ is 0.96.

Fig.1 shows the distribution parameters with their approximated values, and Fig. 4(a) presents the 5%, 50% and 95% percentiles of the probabilistic models using the fitted distribution function and its modeled parameters.

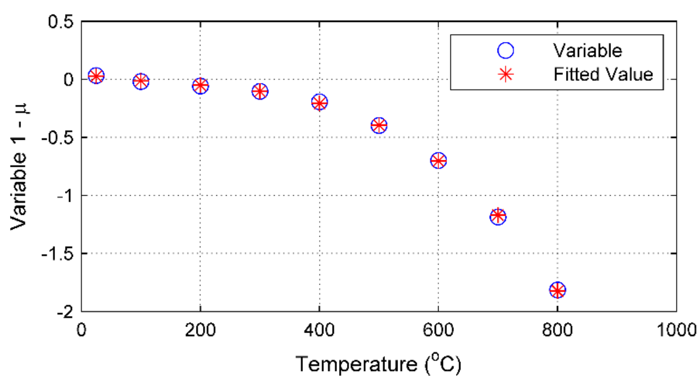

(a) Regression model for variable 1 - μ

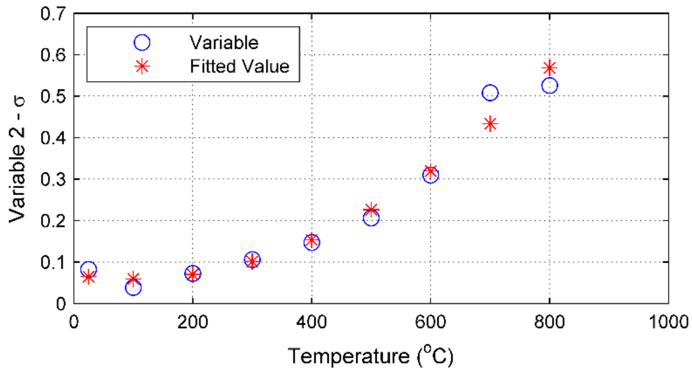

(b) Regression model for variable 2 - σ

Fig. 1. Models to predict the μ (variable 1) and σ (variable 2) for the lognormal distribution fit for the data of compressive strength of normal-strength concrete

Another example for applying the methodology is developing a probabilistic model for the modulus of elasticity for mild steel. The AIC_c estimators and Akaike weights were calculated and presented in Table 2.

Table 2. The *AICc* estimators and Akaike weights for the fitted distribution functions of modulus of elasticity for mild steel

Distribution	AIC_i	w_i	Distribution	AIC_i	w_i
Normal	-165.87	0.03	Loglogistic	-163.75	0.01
Lognormal	-167.93	0.09	Weibull	-171.02	**0.54**
Logistic	-161.49	0.01	Birnbaum-Saunders	-169.74	**0.28**

The two candidate models for modulus of elasticity data were Weibull and Birnbaum-Saunders distributions. A (scale factor) and B (shape factor) are the variables that define Weibull distribution, and they are positive numbers. The best-fit continuous functions for the shape factor, which had a coefficient of determination of 0.89, produced negative or very small values, Fig. 2(b), at temperatures 600°C, 700°C, 800°C, 900°C.

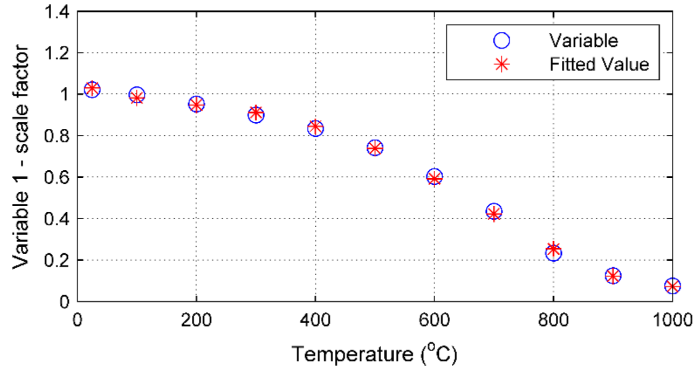

(a) Regression model for variable 1 – scale factor (A)

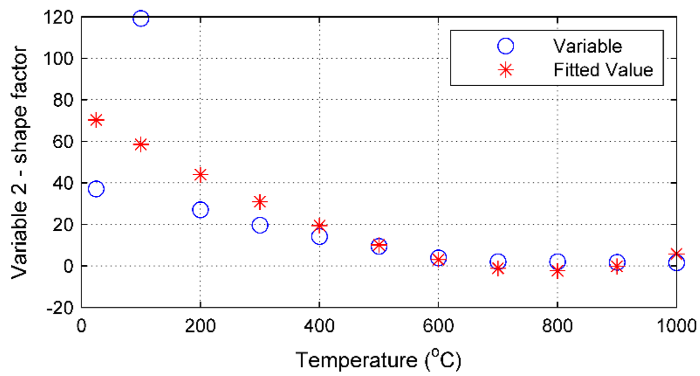

(b) Regression model for variable 2 -shape factor (B)

Fig. 2. Models to predict A (variable 1) with (R^2 = 0.99) and B (variable 2) with (R^2 = 0.89) for the Weibull distribution fit for the data of modulus of elasticity of mild steel

Therefore, the probabilistic model in Fig. 3(a) for the modulus of elasticity assuming that the data followed a Weibull distribution and using the developed models for its parameters failed to present the material property at these temperatures (i.e., 600°C, 700°C, 800°C, 900°C).

This is a preprint draft. The published article can be found at: http://doi.org/10.1002/fam.3116.

Please cite this paper as:
Karaki, G., Naser, M.Z. (2022). An approach for developing probabilistic models for temperature-dependent properties of construction materials from fire tests and small data. *Fire and Materials*. [http://doi.org/10.1002/fam.3116.](http://doi.org/10.1002/fam.3116)

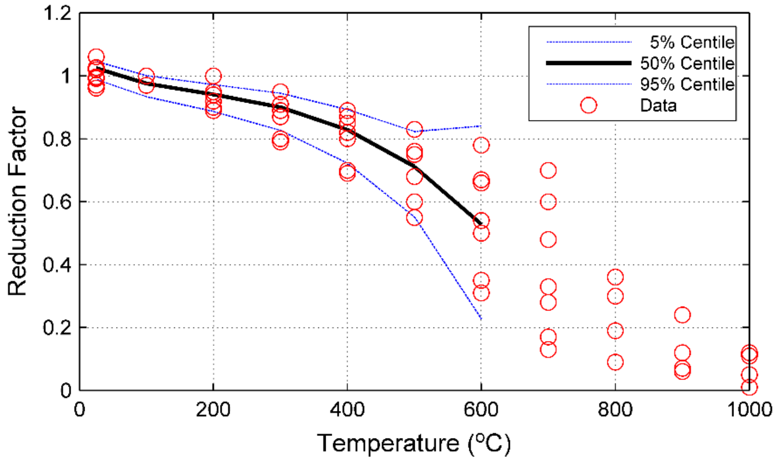

(a) assuming that data points follow Weibull distribution

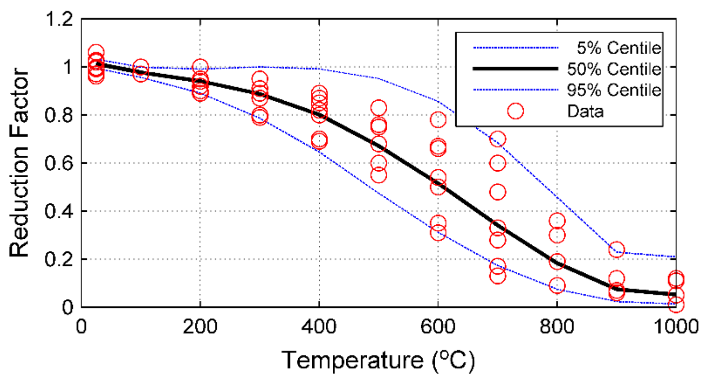

(b) assuming that data points follow Birnbaum-Saunders distribution

Fig. 3. Probabilistic model for modulus of elasticity for the mild steel

Based on this, the second-best candidate, Birnbaum-Saunders distribution, was examined and accepted to model the modulus of elasticity. Eq. 5 documents the fit of the distribution parameters β (scale factor) and γ (shape factor), and Fig. 3(b) shows the (5%, 50%, and 95%) percentiles of the probabilistic model.

$$\beta = -152.3789 + 153.3916 \cdot e^{T_{std}} + 152.8007 \cdot T_{std} - 74.4257 \cdot T_{std}^2 + 17.6276 \cdot T_{std}^3 \quad (5a)$$

$$\gamma = 0.0116 - 0.0527 \cdot T_{std} + 0.9434 \cdot T_{std}^2 \quad (5b)$$

The aforenoted methodology was applied to develop probabilistic models for the thermal and mechanical properties for a collection of construction materials. The followings are the developed models presented by the examined property.

4.1.1 Compressive strength of concrete:

Table 3. Models for the variables defining the probabilistic models for the compressive strength of concrete

Type	Dist.	Model	R^2
NSC	LogNorm.	$\mu = 0.0262 - 0.5103 \cdot T_{std} + 1.3704 \cdot T_{std}^2 - 2.7088 \cdot T_{std}^3$	0.99
		$\sigma = 0.0650 - 0.1172 \cdot T_{std} + 0.6207 \cdot T_{std}^2$	0.96
HSC	Weibull	$A = 1.000 + 0.0789 \cdot T_{std} - 1.4130 \cdot T_{std}^2 + 0.4507 \cdot T_{std}^3$	0.99
		$B = 13.0241 - 29.5246 \cdot T_{std} + 18.7818 \cdot T_{std}^2$	0.79
HPC	LogNorm.	$\mu = -0.0846 + 0.3258 \cdot T_{std} - 1.8333 \cdot T_{std}^2$	0.98
		$\sigma = 0.0931 + 0.2613 \cdot T_{std} + 0.4448 \cdot T_{std}^2$	0.99

The developed probabilistic models are presented in Table 3, and Fig. 4 depicts the attained reduction factor for compressive strength. This factor is defined as the compressive strength at a target temperature normalized by the compressive strength at ambient temperature. The surveyed experimental data provides this factor at different temperatures. The variation of data points at ambient temperature was obtained from the probabilistic models offered by [80]. The median and the 5% and 95% percentiles of reduction factors are shown in Fig. 4. The data and the developed model suggest that the compressive strength of normal-strength concrete has a lower rate of strength loss when compared with high-strength concrete up to the temperatures 400-500°C. However, the strength loss rate was similar at higher temperatures (T>400oC). The leading cause of strength loss above 400°C is the loss of bond between aggregate and cement paste and physio-chemical degradation induced by a rise in temperature, which is similar for both concrete [81]. In general, high-performance concrete shows the same behavior as high-strength concrete. However, a lower rate of strength loss above 400°C was observed; this may depend on the mixture characteristics used to enhance the performance of the concrete.

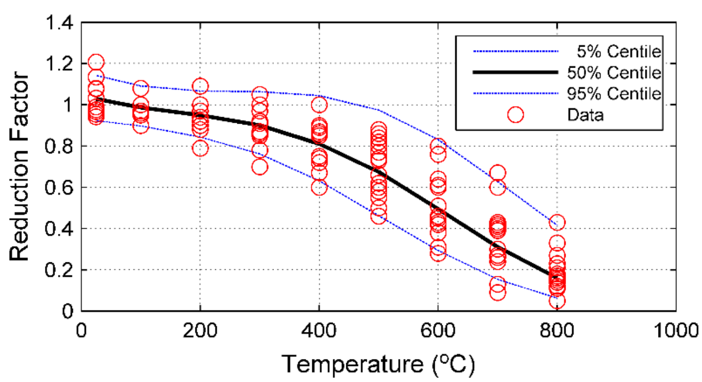

(a) for NSC

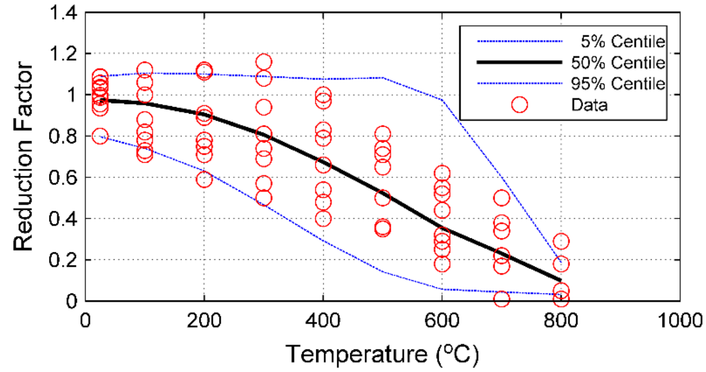

(b) for HSC

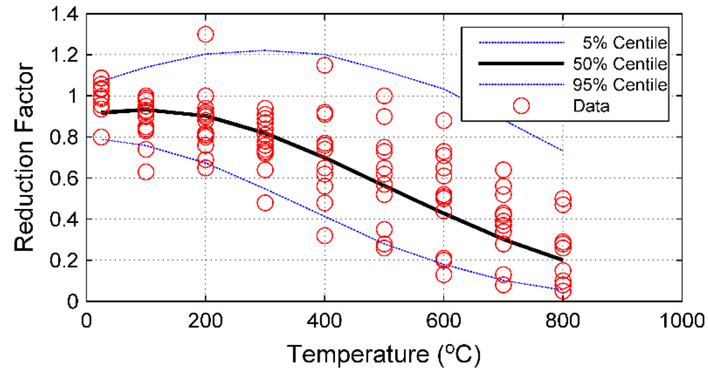

(c) for HPC

Fig. 4. Probabilistic models for the compressive strength of concrete

4.1.2 Modulus of elasticity of concrete

The available data for the concrete modulus of elasticity is presented as a reduction factor. This reduction factor is the modulus of elasticity normalized by the modulus of elasticity at ambient temperature. The variation of data points at ambient temperature was obtained from the probabilistic models offered by [80]. The developed probabilistic models following the explained methodology are documented in Table 4 and Fig. 5.

Table 4. Models for the variables defining the probabilistic models for the modulus of elasticity of concrete

Type	Dist.	Model	R^2
NSC	Weibull	$A = 1.0464 - 0.4376 \cdot T_{std} - 1.6226 \cdot T_{std}^2 + 1.1464 \cdot T_{std}^3$	0.99
		$B = 9.2155 + 12.0703 \cdot T_{std} - 57.4990 \cdot T_{std}^2 + 38.0620 \cdot T_{std}^3$	0.78
HSC	LogNorm.	$\mu = -0.0235 - 0.2987 \cdot T_{std} - 2.5918 \cdot T_{std}^2 + 0.7048 \cdot T_{std}^3$	0.99
		$\sigma = 0.1624 + 0.3306 \cdot T_{std} + 0.2889 \cdot T_{std}^2$	0.72
HPC	Weibull	$A = 1.0726 - 0.8216 \cdot T_{std} - 0.1858 \cdot T_{std}^2$	0.99
		$B = 10.2334 - 17.9296 \cdot T_{std} + 8.6871 \cdot T_{std}^2$	0.74

This is a preprint draft. The published article can be found at: http://doi.org/10.1002/fam.3116.

Please cite this paper as:
Karaki, G., Naser, M.Z. (2022). An approach for developing probabilistic models for temperature-dependent properties of construction materials from fire tests and small data. *Fire and Materials*. http://doi.org/10.1002/fam.3116.

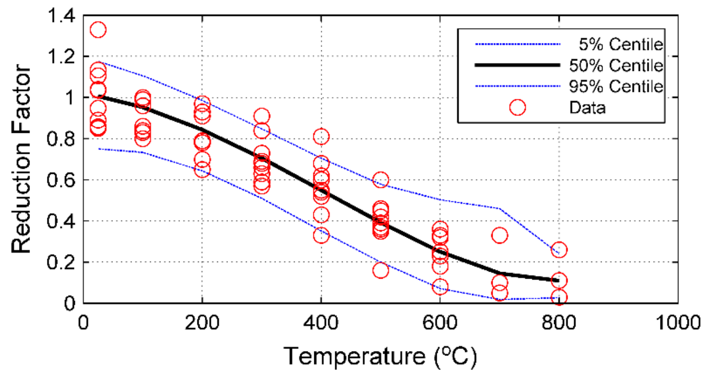

(a) for NSC

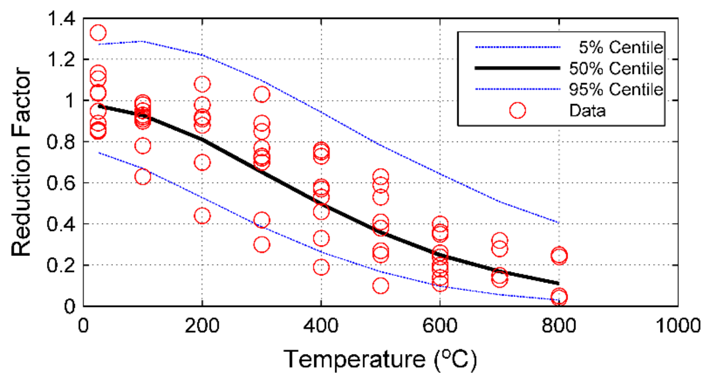

(b) for HSC

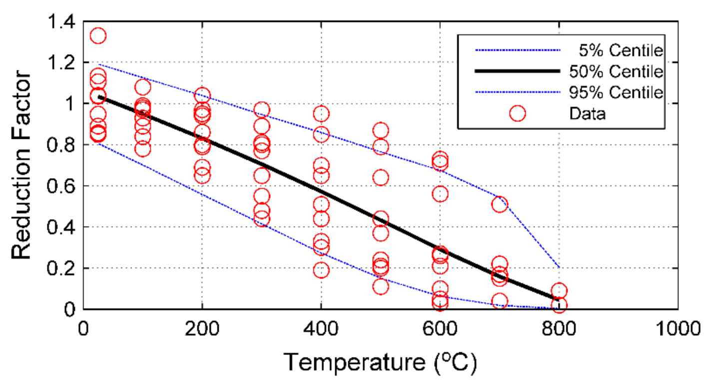

(c) for HPC

Fig. 5. Probabilistic models for the modulus of elasticity of concrete

After examining the data and developed models in Fig. 5, the degradation of the modulus was noticed to occur beyond the temperature of 100°C for normal and high-strength concrete. However, normal-strength concrete retains its modulus better than high-strength concrete at temperatures lower than 400°C. It was observed, from the data, a higher variation of modulus values in high-strength and high-performance concrete within the temperature range [400°C - 600°C]. Furthermore, high-performance concrete showed a constant degradation rate in the modulus values. In general, the strength of concrete did not significantly affect modulus-temperature response.

4.1.3 Thermal conductivity of concrete:

Overall, the scatter in the data points of the thermal conductivity is higher for normal-strength concrete, and this affected the quality of the regression model for one of the parameters defining the probabilistic model for the conductivity of normal-strength concrete, Table 5, and Fig. 6.

Table 5. Models for the variables defining the probabilistic models for thermal conductivity of concrete

Type	Dist.	Model	R^2
NSC	Weibull	$A = 1.7106 - 1.5246 \cdot T_{std} + 0.5222 \cdot T_{std}^2$	0.98
		$B = 4.8809 + 3.6512 \cdot T_{std} - 6.8362 \cdot T_{std}^2$	0.65
HSC	Normal	$\mu = 2.9885 - 6.5231 \cdot T_{std} + 9.5980 \cdot T_{std}^2 - 5.3069 \cdot T_{std}^3$	0.98
		$\sigma = 0.3689 - 0.5716 \cdot T_{std} + 0.4185 \cdot T_{std}^2$	0.88

The lower the mix water content and the denser the microstructure, the higher the conductivity of the hardened concrete; therefore, the conductivity at ambient temperature is higher for high-strength concrete, Fig. 6. In addition, the experimental data showed that the decrease of the thermal conductivity with temperature was higher for high-strength concrete than normal-strength concrete. These observations had been captured by the developed models, as shown in Fig. 6.

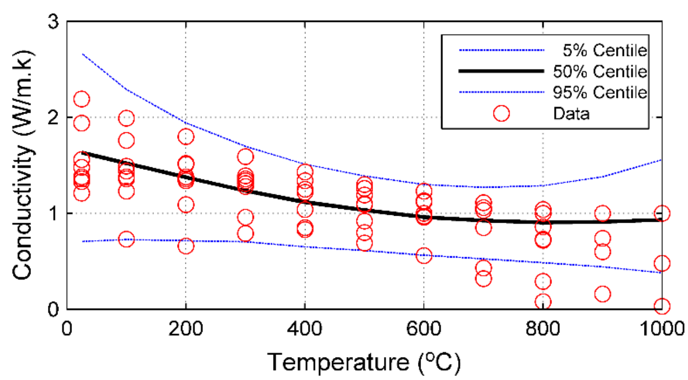

(a) for NSC

This is a preprint draft. The published article can be found at: http://doi.org/10.1002/fam.3116.

Please cite this paper as:
Karaki, G., Naser, M.Z. (2022). An approach for developing probabilistic models for temperature-dependent properties of construction materials from fire tests and small data. *Fire and Materials*. http://doi.org/10.1002/fam.3116.

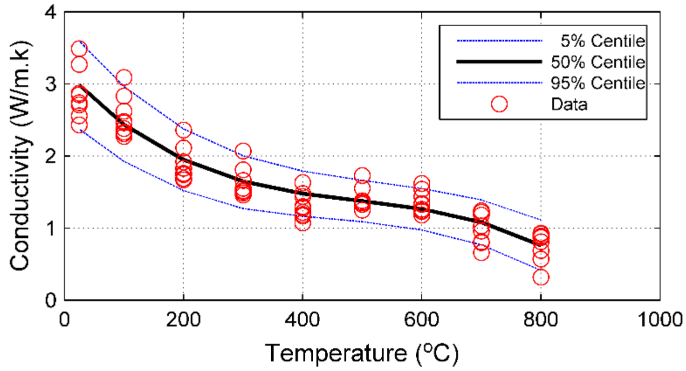

(b) for HSC

Fig. 6. Probabilistic models for the thermal conductivity of concrete

4.1.4 Specific heat of concrete:

The developed probabilistic models for the specific heat of concrete are presented in Table 6. The coefficient of determination for the standard deviation of lognormal distribution used in the probabilistic model for the specific heat of normal-strength concrete was low. This is due to the sudden sharp increase in the specific heat at 700°C stemming from exothermic reactions at the microstructure level often captured by some material models. The developed model predicts a slight rise at 700°C and captures a decrease in specific heat above this temperature. However, fire codes such as Eurocode 2 and the probabilistic model do not capture this sudden increase (see Fig. 7).

Table 6. Models for the variables defining the probabilistic models for the specific heat of concrete

Type	Dist.	Model	R^2
NSC	LogNorm.	$\mu = 6.0345 + 1.1756 \cdot T_{std} - 0.2906 \cdot T_{std}^2$	0.93
		$\sigma = 0.3894 + 0.5245 \cdot T_{std} - 0.6485 \cdot T_{std}^2$	0.15
HSC	LogNorm.	$\mu = 3.4580 - 15.7711 \cdot T_{std} + 25.9841 \cdot T_{std}^2 - 13.1054 \cdot T_{std}^3$	0.85
		$\sigma = 0.1087 - 0.3441 \cdot T_{std} + 0.5616 \cdot T_{std}^2$	0.95

In general, the experimental data for normal-strength concrete and high-strength concrete showed that the specific heat increases as temperature increases. For normal-strength concrete, a sharp rise was observed at 700°C as explained earlier; and for high-strength concrete rises and drops were observed at multiple temperatures; a rise was noticed at 100°C, a drop was seen at 400°C (decrease), and a sharp rise was noticed at 700°C (see Fig. 7). Naus (2010) [81] reviewed concrete behavior and documented that the vaporization of free water happens at about 100°C, the dissociation of $Ca(OH)^2$ happens at about 400°C - 500°C, and the alpha-beta quartz transformation in some aggregates at high temperatures. These may explain these rises and drops in the specific heat values. The behavior, in general, was depicted in the developed probabilistic models, as noted in Fig. 7.

This is a preprint draft. The published article can be found at: http://doi.org/10.1002/fam.3116.

Please cite this paper as:
Karaki, G., Naser, M.Z. (2022). An approach for developing probabilistic models for temperature-dependent properties of construction materials from fire tests and small data. *Fire and Materials*. http://doi.org/10.1002/fam.3116.

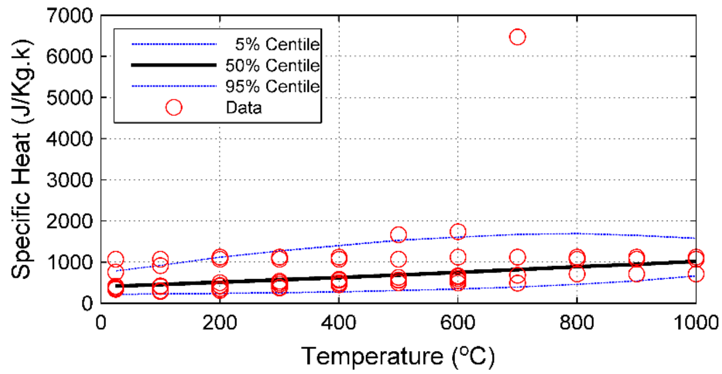

(a) for NSC

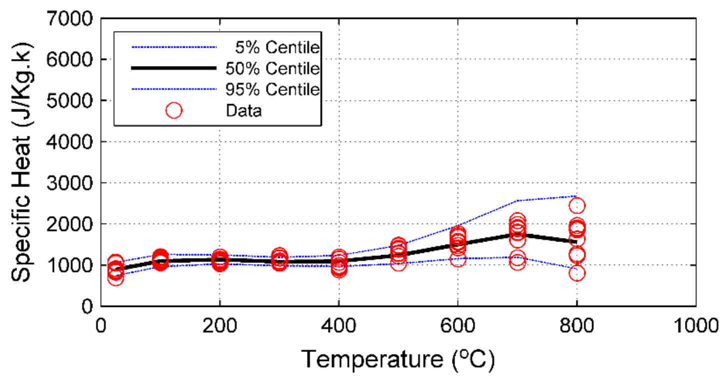

(b) HSC

Fig. 7. Probabilistic models for the specific heat of concrete

4.1.5 Yield strength of steel:

The experimental data for the yield strength was obtained as reduction factors. The variability in the data points at ambient temperature was obtained from [82]. In general, the variation in the steel data is less than that of the concrete, reflecting the homogenous nature of steel as opposed to concrete. Following the data for mild steel (MS) and high-strength steel, the yield strength's apparent loss starts at temperatures exceeding 300°C, Fig. 8, which the model described in Table 7 depicts.

Table 7. Models for the variables defining the probabilistic models for the yield strength of steel

Type	Dist.	Model	R^2
MS	Weibull	$A = -313.6871 + 314.7100 \cdot e^{T_{std}} + 313.7510 \cdot T_{std} - 151.1840 \cdot T_{std}^2 + 35.4004 \cdot T_{std}^3$	0.99
		$B = 28.8804 - 65.9409 \cdot T_{std} + 40.8658 \cdot T_{std}^2$	0.87
HSS	Weibull	$A = -261.9452 + 262.9604 \cdot e^{T_{std}} + 262.4889 \cdot T_{std} - 127.8017 \cdot T_{std}^2 + 30.5845 \cdot T_{std}^3$	0.99
		$B = 27.2539 - 85.5850 \cdot T_{std} + 93.7015 \cdot T_{std}^2 - 33.0861 \cdot T_{std}^3$	0.95
CFS	Weibull	$A = -83.0998 + 84.0975 \cdot e^{T_{std}} + 84.2817 \cdot T_{std} - 43.8306 \cdot T_{std}^2 + 11.7404 \cdot T_{std}^3$	0.99
		$B = -6.7527 \cdot 10^3 + 6.8234 \cdot 10^3 \cdot e^{T_{std}} + 6.4732 \cdot 10^3 \cdot T_{std} - 2.7265 \cdot 10^3 \cdot T_{std}^2 + 498.9117 \cdot T_{std}^3$	0.94

Based on the models in Fig. 8, MS had a reduction factor of 0.91, 0.48, 0.08 at 300°C, 600°C, and 800°C, respectively. HSS had a reduction factor of 0.90, 0.42, 0.06 at the same temperatures, whereas CFS had reduction factors of 0.85, 0.34, 0.06. Therefore, the yield strength slightly depends on the type of material. Furthermore, high-strength and cold-formed steel had higher loss rates than mild steel.

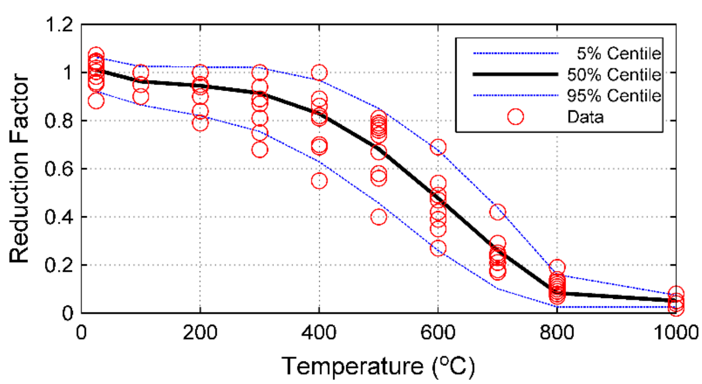

(a) For MS

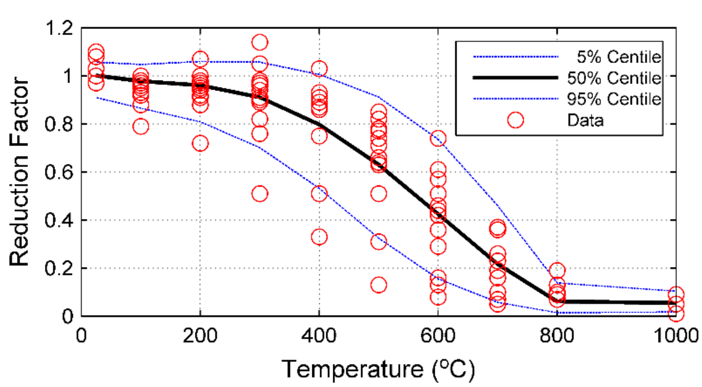

This is a preprint draft. The published article can be found at: http://doi.org/10.1002/fam.3116.

Please cite this paper as:
Karaki, G., Naser, M.Z. (2022). An approach for developing probabilistic models for temperature-dependent properties of construction materials from fire tests and small data. *Fire and Materials*. http://doi.org/10.1002/fam.3116.

(b) HSS

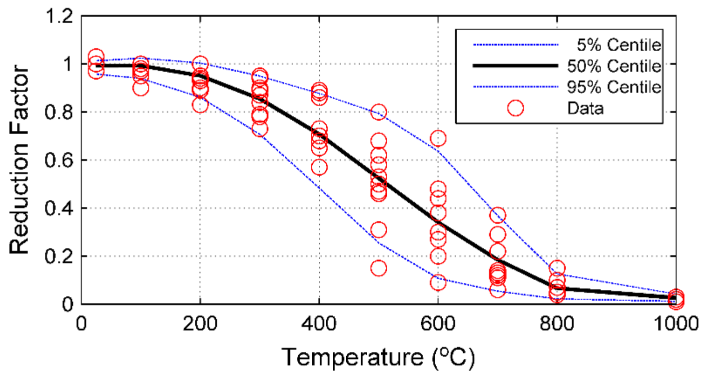

(c) CFS

Fig. 8. Probabilistic models for the yield strength of steel

4.1.6 Modulus of elasticity of steel:

After examining the data for the reduction factor of yield strength and modulus of elasticity, as can be seen in Fig. 8 and Fig. 9, it can be noticed that the variation in the data points is more significant at temperatures 400°C, 500°C, and 600°C. Furthermore, the variability in the data points at ambient temperature was obtained from [82]. The developed probabilistic models are described in Table 8, and they capture this variation dependency on the temperature.

Table 8. Models for the variables defining the probabilistic models for the modulus of elasticity of steel

Type	Dist.	Model	R^2
MS	Birnbaum-Saunders	$\beta = -152.3789 + 153.3916 \cdot e^{T_{std}} + 152.8007 \cdot T_{std} - 74.4257 \cdot T_{std}^2 + 17.6276 \cdot T_{std}^3$	0.99
		$\gamma = 0.0116 - 0.0527 \cdot T_{std} + 0.9434 \cdot T_{std}^2$	0.92
HSS	Weibull	$A = -127.4544 + 128.4695 \cdot e^{T_{std}} + 128.3550 \cdot T_{std} - 63.9892 \cdot T_{std}^2 + 15.8965 \cdot T_{std}^3$	0.99
		$B = 36.8780 - 132.8149 \cdot T_{std} + 161.8747 \cdot T_{std}^2 - 61.2240 \cdot T_{std}^3$	0.98
CFS	LogNorm.	$\mu = 3.6773 - 3.6953 \cdot e^{T_{std}} - 2.9402 \cdot T_{std} - 3.7561 \cdot T_{std}^2 + 0.9260 \cdot T_{std}^3$	0.99
		$\sigma = 0.0225 + 0.2367 \cdot T_{std} + 0.3619 \cdot T_{std}^2$	0.57

As one examines Fig. 9, the modulus of elasticity for mild steel undergoes a lower loss than high-strength steel and cold-formed steel.

This is a preprint draft. The published article can be found at: http://doi.org/10.1002/fam.3116.

Please cite this paper as:
Karaki, G., Naser, M.Z. (2022). An approach for developing probabilistic models for temperature-dependent properties of construction materials from fire tests and small data. *Fire and Materials*. http://doi.org/10.1002/fam.3116.

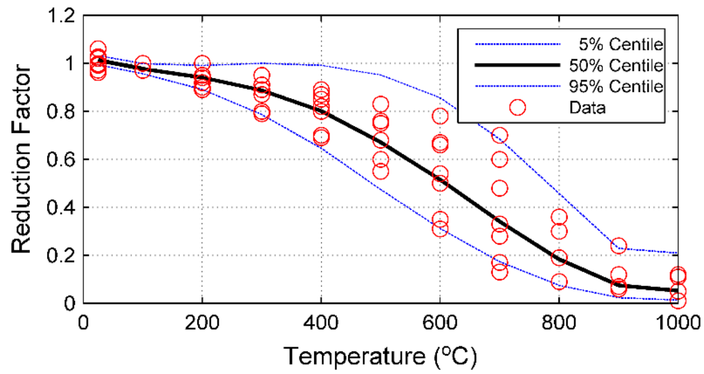

(a) for MS

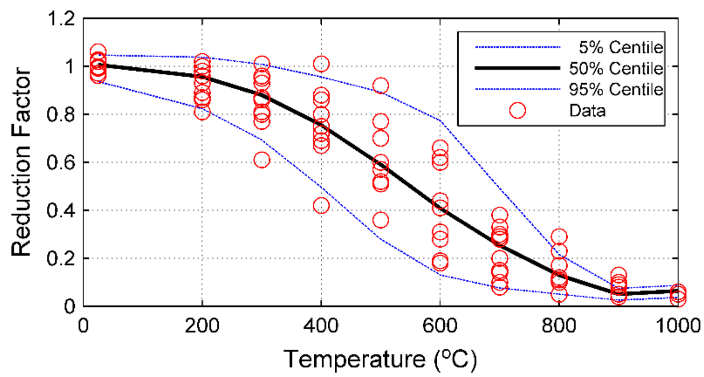

(b) for HSS

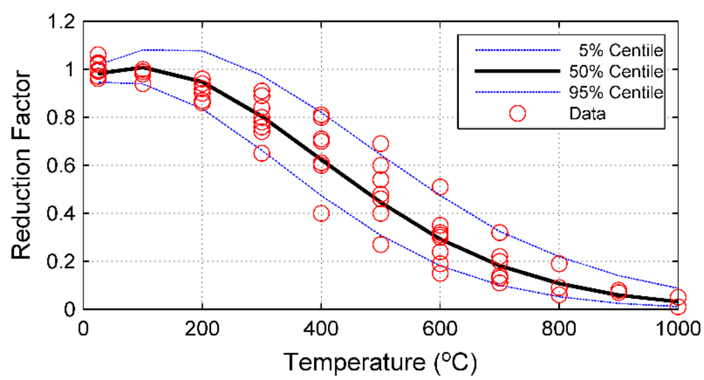

(c) for CFS

Fig. 9. Probabilistic models for the modulus of elasticity of steel

4.1.7 Thermal conductivity of steel:

The probabilistic models for the thermal conductivity of steel are described in Table 9 and depicted in Fig. 10. The number of data points is small for high-strength concrete, which affects the choice of the distribution function used in the probabilistic model. Normal

This is a preprint draft. The published article can be found at: http://doi.org/10.1002/fam.3116.

Please cite this paper as:
Karaki, G., Naser, M.Z. (2022). An approach for developing probabilistic models for temperature-dependent properties of construction materials from fire tests and small data. *Fire and Materials*. http://doi.org/10.1002/fam.3116.

distribution was chosen, and consequently, the quality of the fit was affected by this choice and the limited number of data points. It can be seen from Fig. 10 that thermal conductivity decreases with temperature for the mild steel and high-strength steel. Furthermore, the decrease is higher in mild steel, but one must keep in mind that the data of high-strength steel is much-limited opposite to mild steel.

Table 9. Models for the variables defining the probabilistic models for thermal conductivity of steel

Type	Dist.	Model	R^2
MS	LogNorm.	$\mu = 3.9373 - 0.6906 \cdot T_{std} + 0.1568 \cdot T_{std}^2$	0.99
		$\sigma = 0.0408 + 0.1664 \cdot T_{std} - 0.0182 \cdot T_{std}^2$	0.91
HSS	Norm	$\mu = 34.5748 - 1.9970 \cdot T_{std} - 0.8403 \cdot T_{std}^2$	0.72
		$\sigma = 3.0993 + 0.3630 \cdot T_{std}$	--

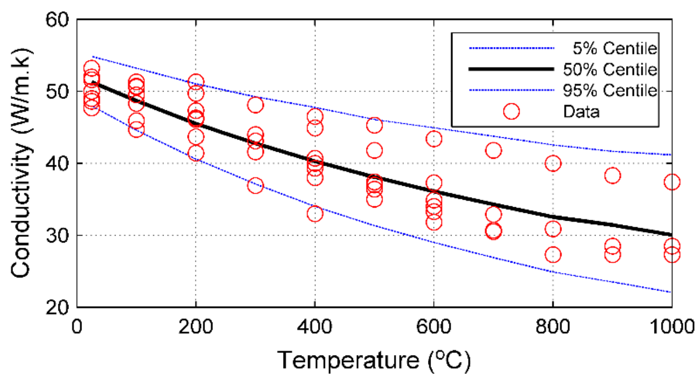

(a) for MS

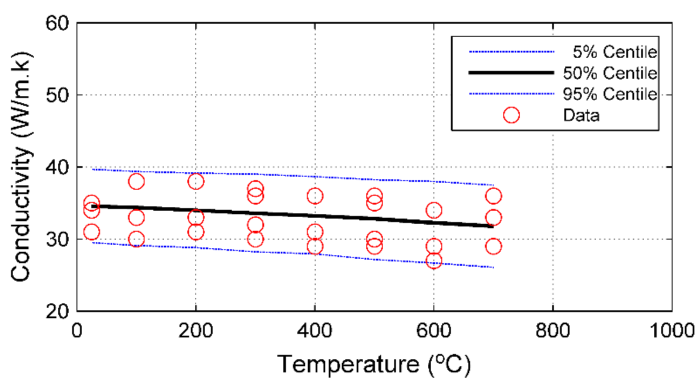

(b) for HSS

Fig. 10. Probabilistic models for thermal conductivity of steel

4.1.8 Specific heat of steel:

The data points for mild and high-strength steel's specific heat were examined. The number of data points for high-strength steel is also small, affecting the distribution function's choice. A lognormal distribution is chosen for the probabilistic model for high-strength steel. Table 10 presents the probabilistic model for the specific heat, and the models are depicted in Fig. 11.

Table 10. Models for the variables defining the probabilistic models for the specific heat of steel

Type	Dist.	Model	R^2
MS	LogNorm.	$\mu = 6.1412 + 0.0199 \cdot T_{std} + 3.1816 \cdot T_{std}^2 - 2.9890 \cdot T_{std}^3$	0.83
		$\sigma = 0.0602 + 0.0336 \cdot T_{std} + 0.4454 \cdot T_{std}^2 - 0.4799 \cdot T_{std}^3$	0.87
HSS	LogNorm.	$\mu = 5.9713 + 1.9821 \cdot T_{std} - 8.9057 \cdot T_{std}^2 + 16.5952 \cdot T_{std}^3 - 8.7918 \cdot T_{std}^4$	0.97
		$\sigma = 0.0713 + 0.1769 \cdot T_{std} - 0.1645 \cdot T_{std}^2$	--

Fig. 11 depicts that specific heat increases with temperature. Following the data of mild steel, a peak is noticed at 700°C. The same observation is noticed for high-strength steel. The probabilistic model predicts this behavior for mild- and high-strength steel. However, only two data points were available for high-strength steel to model its behavior above 700°C.

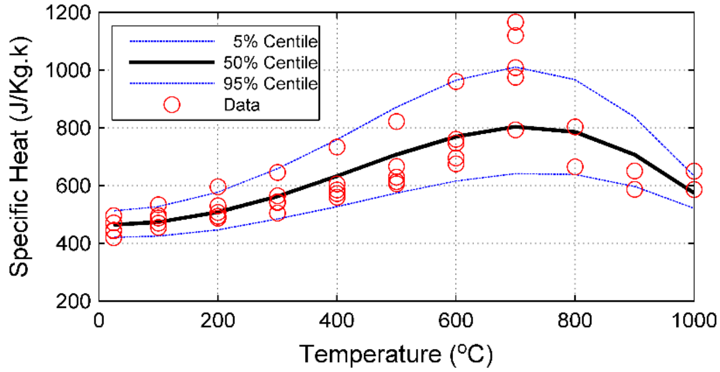

(a) for MS

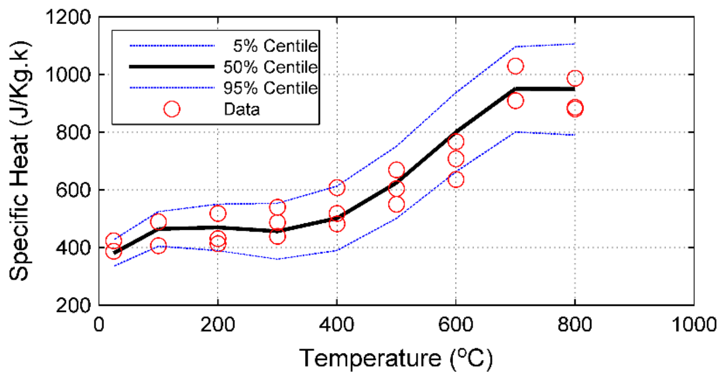

(b) for HSS

Fig. 11. Probabilistic models for specific heat of steel

4.2 Practical Applications of Developed Models

Closed-form equations are determined for the distribution parameters of material properties as a function of temperature. During the probabilistic analysis, the temperature-dependent distribution parameters are evaluated, and probability distribution functions are created. A user-input percentile is used to obtain a point on the created probability distribution function and used in the thermo-mechanical analysis of the structural element. The derived relationships for the material properties at elevated temperatures are valid in the temperature ranges covered by the surveyed experimental data. Furthermore, their development framework is flexible in that new test data can be added, and the validity of the developed material models can be constantly extended.

4.3 Model Comparisons

The models developed in this paper are compared with models developed by [18,19]. The methodology in [18,19] used artificial neural networks to describe the data, whereas, in this study, the data is fitted using a probabilistic approach, as explained earlier. Fig. 12 presents the 50% percentile of the developed probabilistic models (Prop. Model) and the

Artificial Neural Network-based models (ANN model) for NSC and HSC; Fig. 13 presents the 50% percentile of the developed probabilistic models (Prop. Model) and the Artificial Neural Network-based models (ANN model) for MS and HSS. The material types that had enough data points to develop temperature-dependent material models for all the considered thermal and mechanical properties are used in this comparison. Furthermore, the material models of ASCE, 1992 [10], Eurocode 2, 2004 [4], and Eurocode 3, 2005 [5] with the mean value of the experimental data are presented in Fig. 12 and Fig. 13. Since most material models in the fire standards are based on averages of experimental data for NSC and MS, it can be seen that there is a general agreement between the different models for most NSC and MS material properties, Fig. 12 and Fig. 13.

It should be noted that the approach to derive Prop. model examines different probability distribution functions for the data modeling, and both Prob. and ANN models are developed using more recent experimental data sets than standards and codes. Moreover, it is noticed from the experimental data and the derived models that the strength of the material has a significant effect on the material properties, i.e., strength/yield, conductivity, and specific heat. For example, the compact microstructure of HSC does not allow moisture to escape. This causes a buildup in the pore pressure, which accelerates the development of microcracks and, consequently, causes the loss of strength. This faster deterioration of strength in HSC is depicted in the derived models, Fig. 12(a). Furthermore, the thermal conductivity of HSC is expected to be higher than that of NSC due to the different types of binders used in HSC and its low water-to-cement ratio, and this behavior is captured in the developed models in Fig. 12(c). High-strength steels are made by adding different types of alloys that affect the fire resistance property of steel [46]; the experimental data and developed models in Fig. 13 indicate such changes in material behavior at elevated temperatures. The observations above support the need to derive generalized and probabilistic material models for the more modern construction materials that vary in strength and type.

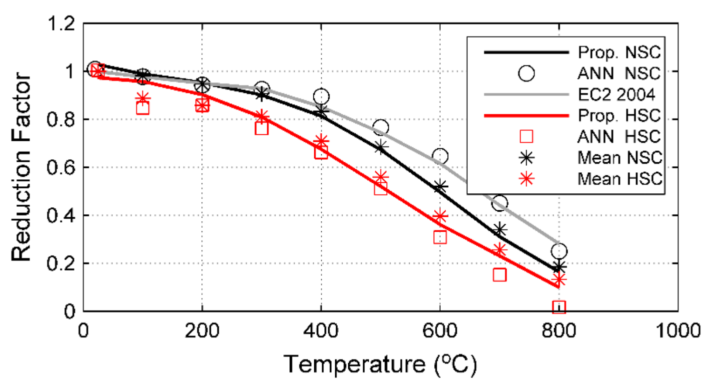

(a) Reduction factor for compressive strength

This is a preprint draft. The published article can be found at: http://doi.org/10.1002/fam.3116.

Please cite this paper as:
Karaki, G., Naser, M.Z. (2022). An approach for developing probabilistic models for temperature-dependent properties of construction materials from fire tests and small data. *Fire and Materials*. http://doi.org/10.1002/fam.3116.

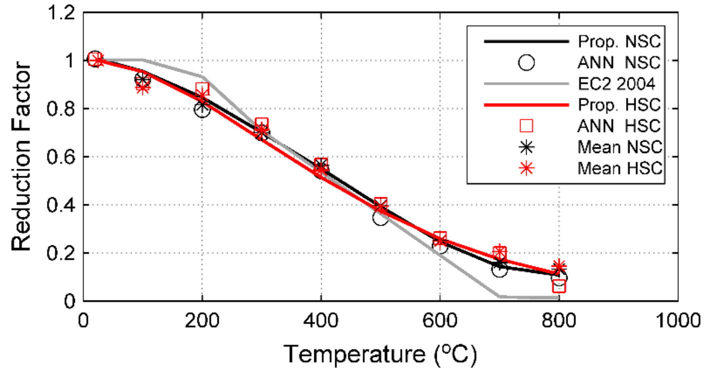

(b) Reduction factor for modulus of elasticity

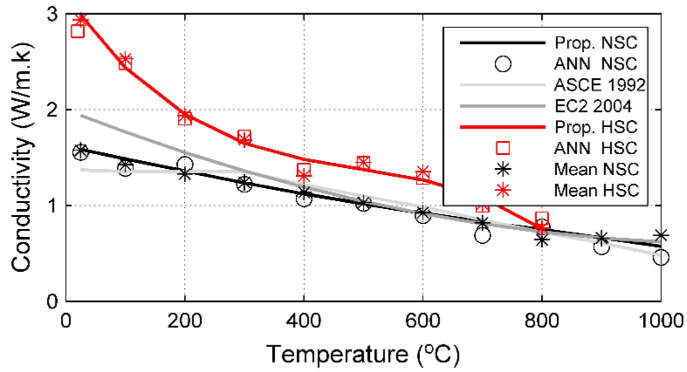

(c) Thermal conductivity

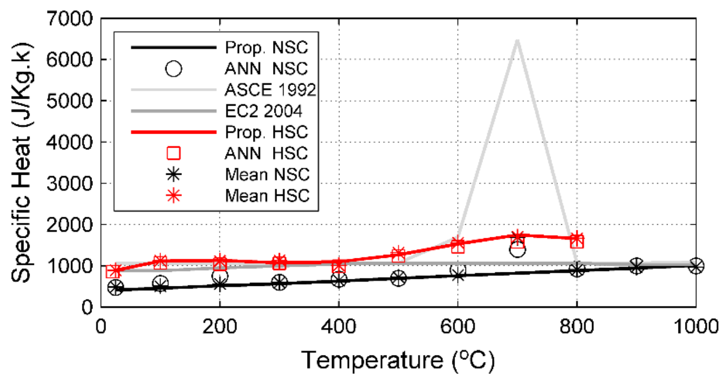

(d) Specific Heat

Fig. 12: Model comparison for the thermal and mechanical properties of concrete

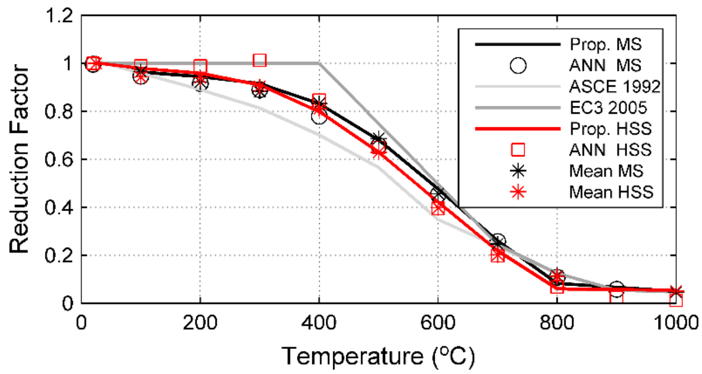

(a) Reduction factor for yield strength

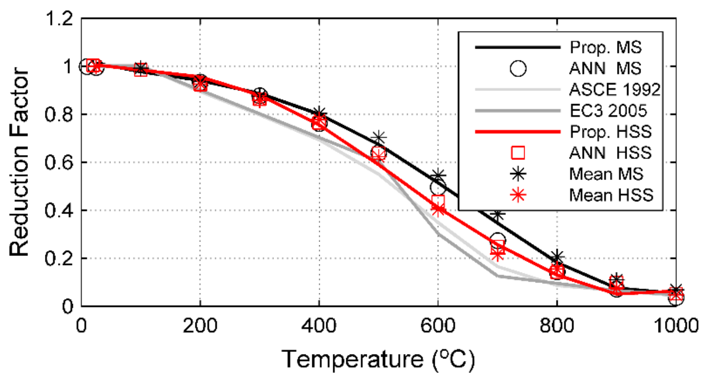

(b) Reduction factor for modulus of elasticity

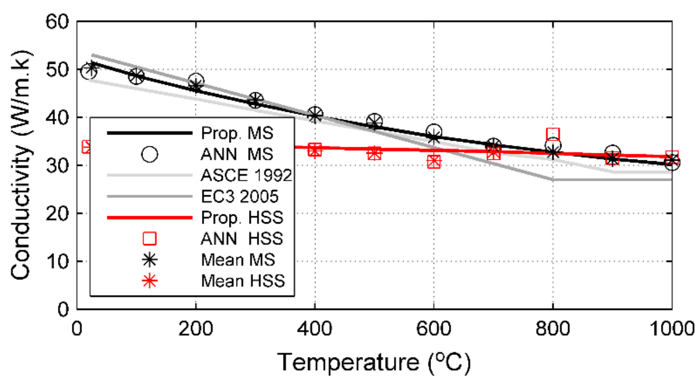

(c) Thermal conductivity

This is a preprint draft. The published article can be found at: http://doi.org/10.1002/fam.3116.

Please cite this paper as:
Karaki, G., Naser, M.Z. (2022). An approach for developing probabilistic models for temperature-dependent properties of construction materials from fire tests and small data. *Fire and Materials*. http://doi.org/10.1002/fam.3116.

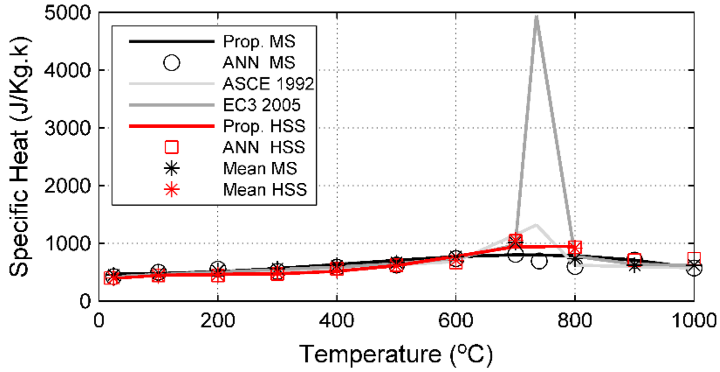

(d) Specific heat

Fig. 13: Model comparison for the thermal and mechanical properties of steel

5. Conclusions

The examined material properties are temperature-dependent, and the experimental data show a large variability for their values. Therefore, there is a need for probabilistic models to quantify the observed scatter in data at elevated temperatures. The availability of probabilistic material models in structural fire engineering facilitates probabilistic performance-based fire engineering and allows a detailed evaluation of structural fire reliability. This study presents a methodology to develop temperature-dependent probabilistic material models. The approach analyzes a comprehensive list of surveyed experimental data at different temperature groups, tests the goodness of fit for a number of distributions, and derives continuous functions to quantify temperature-dependent parameters of the fitted distribution functions. The paper provides probabilistic models for the thermal and mechanical properties for normal-strength, high-strength, and high-performance concrete and mild, high-strength, and cold-formed steels. Furthermore, the 50% percentile of developed probabilistic models were compared with ANN developed models for the concrete and steel temperature-dependent material properties; both models showed a general agreement. The proposed models to quantify uncertainties in concrete and steel temperature-dependent material properties can be used to complete the reliability analysis, derive safety factors and perform sensitivity analysis for the fire design of buildings.

Appendix

A sample code in MATLAB to create the data points for the material properties using the developed probabilistic models.

```
% Creation of material property data points for a probabilistic study
% Sample code Matlab

%% candidate distributions
Distributions={'Birnbaumsaunders' 'loglogistic' 'logistic' ...
     'lognormal' 'Normal' 'Weibull'};
```

```
DistVar1={'pd.beta' 'pd.mu' 'pd.mu' ...
    'pd.mu' 'pd.mu' 'pd.A'};
DistVar2={'pd.gamma' 'pd.sigma' 'pd.sigma'...
     'pd.sigma' 'pd.sigma' 'pd.B'};

%% Example: create probabilistic model for compressive strength of
normal strength concrete
j=4; % follwoing the output of the study - best fit is the lognormal
distribution
%% Regression models
% a are regression coefficients provided in the study for the first
variable defining distribution function
% b are regression coefficients provided in the study for the second
variable defining distribution function
a=[0.0262 -0.5103 1.3704 -2.7088]';
b=[0.065 -0.1172 0.6207]';
% Regression terms, these changes following terms given in the study
% T is the array of examined temperatures
T=[25 100 200 300 400 500 600 700 800];
Tstd = (T - min(T))/(max(T)-min(T));
Xa = [ones(size(Tstd))' (Tstd.^1)' (Tstd.^2)' (Tstd.^3)'];
Xb = [ones(size(Tstd))' (Tstd.^1)' (Tstd.^2)' ];
% Approximated distribution parameters for examined temperatures
var1=Xa*a; var2=Xb*b;

%% Realization of samples of the examined property using the derived
model
NumSamples=10000;

for i=1:size(T,2)
    PropData(:,i)=
random(Distributions{j},var1(i),var2(i),NumSamples,1);
end

PropData50=quantile(PropData,0.5,1);
```

Data Availability

Data, models, or code that support the findings of this study are available from the corresponding author upon reasonable request.

References

[1] V.K.R. Kodur, A. Agrawal, An approach for evaluating residual capacity of reinforced concrete beams exposed to fire, Eng. Struct. 110 (2016) 293–306. https://doi.org/10.1016/j.engstruct.2015.11.047.

[2] ASCE, Structural Fire Protection: Manual of Practice, 1993.

[3] ACI, Guide for Determining the Fire Endurance of Concrete Elements, ACI-216–89, Detroit, MI, 1989.

[4] Eurocode2, design of concrete structures, Part1-2: General rules-structural fire

design, UK, 2004.

[5] Eurocode3, EN 1993-1-2:Design of Steel Structures. Part 1-2: General Rules-Structural Fire Design, UK, 2005.

[6] T.Z. Harmathy, Fire Safety Design and Concrete, Longman Scientific and Technical, Harlow, UK, 1993.

[7] I.D. Bennetts, Report No. MRL/PS23/81/001, Clayton, Australia, 1981.

[8] U. Schneider, Properties of Materials at High Temperatures—Concrete, Kassel, Germany, 1985.

[9] Y. Anderberg, Properties of Materials at High Temperatures—Steel, Lund, Sweden, 1983.

[10] ASCE, Structural Fire Protection - ASCE Manuals and Reports on Engineering, New York, NY, 1992.

[11] P.L. T., High-strength concrete at high temperature—an overview, in: 6th Int. Symp. Util. High Strength/High Perform. Concr., Leipzig, Germany, 2002: pp. 501–518.

[12] M.Z. Naser, V.A. Uppala, Properties and material models for construction materials post exposure to elevated temperatures, Mech. Mater. 142 (2020). https://doi.org/10.1016/j.mechmat.2019.103293.

[13] ACI216.1, Standard Method for Determining Fire Resistance of Concrete and Masonry Construction Assemblies, 2014.

[14] ECS, EN 1993-1-2: Design of steel structures. Part 1-2: General rules-structural fire design, ECS, Brussels, 2005.

[15] W. Khaliq, Performance characterization of high performance concretes under fire conditions, Michigan State University, 2012.

[16] G.L. Bai, N.J. Du, Y.Z. Xu, C.G. Qin, Study on the Thermal Properties of Hollow Shale Blocks as Self-Insulating Wall Materials, Adv. Mater. Sci. Eng. (2017). https://doi.org/10.1155/2017/9432145.

[17] K.D. Hertz, Reinforcement data for fire safety design, Mag. Concr. Res. (2004).

[18] M.Z. Naser, Properties and material models for modern construction materials at elevated temperatures, Comput. Mater. Sci. 160 (2019) 16–29. https://doi.org/10.1016/j.commatsci.2018.12.055.

[19] M.Z. Naser, Properties and material models for common construction materials at elevated temperatures, Constr. Build. Mater. 215 (2019) 192–206. https://doi.org/10.1016/j.conbuildmat.2019.04.182.

[20] A.F. Bingöl, R. Gül, Effect of elevated temperatures and cooling regimes on normal strength concrete, Fire Mater. 33 (2009) 79–88. https://doi.org/10.1002/fam.987.

[21] R. Van Coile, D. Hopkin, D. Lange, Guest Editorial: Probabilistic Methods in Fire Safety Engineering, Fire Technol. 55 (2019) 1107–1109. https://doi.org/10.1007/s10694-019-00874-0.

[22] R. Van Coile, D. Hopkin, D. Lange, G. Jomaas, L. Bisby, The Need for Hierarchies of Acceptance Criteria for Probabilistic Risk Assessments in Fire Engineering, Fire Technol. 55 (2019) 1111–1146. https://doi.org/10.1007/s10694-018-0746-7.

[23] M. Shrivastava, A.K. Abu, R.P. Dhakal, P.J. Moss, Severity Measures and Stripe Analysis for Probabilistic Structural Fire Engineering, Fire Technol. 55 (2019) 1147–1173. https://doi.org/10.1007/s10694-018-0799-7.

[24] T. Gernay, N.E. Khorasani, M. Garlock, Fire Fragility Functions for Steel Frame Buildings: Sensitivity Analysis and Reliability Framework, Fire Technol. 55 (2019) 1175–1210. https://doi.org/10.1007/s10694-018-0764-5.

[25] A. Der Kiureghian, O. Ditlevsen, Aleatory or epistemic? Does it matter?, Struct. Saf. 31 (2009) 105–112. https://doi.org/10.1016/j.strusafe.2008.06.020.

[26] T. Gernay, N. Elhami Khorasani, M. Garlock, Fire fragility curves for steel buildings in a community context: A methodology, Eng. Struct. 113 (2016) 259–276. https://doi.org/10.1016/j.engstruct.2016.01.043.

[27] Q. Guo, A.E. Jeffers, Finite-Element Reliability Analysis of Structures Subjected to Fire, J. Struct. Eng. 141 (2015) 04014129. https://doi.org/10.1061/(asce)st.1943-541x.0001082.

[28] M. Heidari, F. Robert, D. Lange, G. Rein, Probabilistic Study of the Resistance of a Simply-Supported Reinforced Concrete Slab According to Eurocode Parametric Fire, Fire Technol. 55 (2019) 1377–1404. https://doi.org/10.1007/s10694-018-0704-4.

[29] N.E. Khorasani, P. Gardoni, M. Garlock, Probabilistic Fire Analysis: Material Models and Evaluation of Steel Structural Members, J. Struct. Eng. 141 (2015) 04015050. https://doi.org/10.1061/(asce)st.1943-541x.0001285.

[30] R. Qureshi, S. Ni, N. Elhami Khorasani, R. Van Coile, D. Hopkin, T. Gernay, Probabilistic Models for Temperature-Dependent Strength of Steel and Concrete, J. Struct. Eng. 146 (2020) 04020102. https://doi.org/10.1061/(asce)st.1943-541x.0002621.

[31] B. Jovanović, N.E. Khorasani, T. Thienpont, R.K. Chaudhary, R. Van Coile, Probabilistic models for thermal properties of concrete, in: Proc. 11th Int. Conf.

Struct. Fire, The University of Queensland, Brisbane, Australia, 2020. https://doi.org/10.14264/363ff91.

[32] G. Karaki, R.A. Hawileh, V.K.R. Kodur, Probabilistic-Based Approach for Evaluating the Thermal Response of Concrete Slabs under Fire Loading, J. Struct. Eng. 147 (2021) (ASCE)ST.1943-541X.0003039. https://doi.org/10.1061/(ASCE)ST.1943-541X.0003039.

[33] K.-Y. Shin, S.-B. Kim, J.-H. Kim, M. Chung, P.-S. Jung, Thermo-physical properties and transient heat transfer of concrete at elevated temperatures, Nucl. Eng. Des. 212 (2002) 233–241. https://doi.org/10.1016/S0029-5493(01)00487-3.

[34] D. Bentz, K. Prasad, Thermal performance of fire resistive materials I. Characterization with respect to thermal performance models, Gaithersburg, MD., 2007.

[35] G.-Q. Li, S.-C. Jiang, Y.-Z. Yin, K. Chen, M.-F. Li, Experimental Studies on the Properties of Constructional Steel at Elevated Temperatures, J. Struct. Eng. 129 (2003) 1717–1721. https://doi.org/10.1061/(ASCE)0733-9445(2003)129:12(1717).

[36] J. Outinen, P. Mäkeläinen, Mechanical properties of structural steel at elevated temperatures and after cooling down, Fire Mater. 28 (2004) 237–251. https://doi.org/10.1002/fam.849.

[37] Z.P. Bazant, M.F. Kaplan, Concrete at high temperatures: material properties and mathematical models, Prentice Hall, 1996.

[38] E. Mecozzi, B. Zhao, Development of stress–strain relationships of cold-formed lightweight steel at elevated temperatures, in: 4th Eur. Conf. Steel Compos. Struct., 2005: pp. 41–49.

[39] W. Khaliq, V. Kodur, Thermal and mechanical properties of fiber reinforced high performance self-consolidating concrete at elevated temperatures, Cem. Concr. Res. 41 (2011) 1112–1122. https://doi.org/10.1016/j.cemconres.2011.06.012.

[40] V.K.R. Kodur, M.A. Sultan, Effect of Temperature on Thermal Properties of High-Strength Concrete, J. Mater. Civ. Eng. 15 (2003) 101–107. https://doi.org/10.1061/(ASCE)0899-1561(2003)15:2(101).

[41] T.T. Lie, V.K. Kodur, Thermal and mecanical properties of steel-fibre-reinforced concrete at elevated temperatures, Can. J. Civ. Eng. 23 (1996) 511–517.

[42] J. Xiao, Q. Xie, W. Xie, Study on high-performance concrete at high temperatures in China (2004–2016) - An updated overview, Fire Saf. J. 95 (2018) 11–24. https://doi.org/10.1016/j.firesaf.2017.10.007.

[43] J. Xiao, Z. Li, Back-analysis and variability of the thermal conductivity of high strength concrete under high temperatures, J. Archit. Civ. Eng. 31 (2014) 44-49 in

Chinese.

[44] I.-R. Choi, K.-S. Chung, D.-H. Kim, Thermal and mechanical properties of high-strength structural steel HSA800 at elevated temperatures, Mater. Des. 63 (2014) 544–551. https://doi.org/10.1016/j.matdes.2014.06.035.

[45] J.L. Rempe, D.L. Knudson, High temperature thermal properties for metals used in LWR vessels, J. Nucl. Mater. 372 (2008) 350–357. https://doi.org/10.1016/j.jnucmat.2007.03.268.

[46] V.K.R. Kodur, T.Z. Harmathy, Properties of Building Materials, in: SFPE Handb. Fire Prot. Eng., Springer New York, New York, NY, 2016: pp. 277–324. https://doi.org/10.1007/978-1-4939-2565-0_9.

[47] M.-X. Xiong, J.Y.R. Liew, Mechanical behaviour of ultra-high strength concrete at elevated temperatures and fire resistance of ultra-high strength concrete filled steel tubes, Mater. Des. 104 (2016) 414–427. https://doi.org/10.1016/j.matdes.2016.05.050.

[48] L.T. Phan, High-strength concrete at high temperature-an overview, in: 6th Int. Symp. Util. High Strength/High Perform. Concr., Leipzig, Germany, 2002: pp. 501–518.

[49] G.M. Chen, Y.H. He, H. Yang, J.F. Chen, Y.C. Guo, Compressive behavior of steel fiber reinforced recycled aggregate concrete after exposure to elevated temperatures, Constr. Build. Mater. 71 (2014) 1–15. https://doi.org/10.1016/j.conbuildmat.2014.08.012.

[50] R.T. Way, K. Wille, Effect of Heat-Induced Chemical Degradation on the Residual Mechanical Properties of Ultrahigh-Performance Fiber-Reinforced Concrete, J. Mater. Civ. Eng. 28 (2016) 04015164. https://doi.org/10.1061/(ASCE)MT.1943-5533.0001402.

[51] M. Behloul, G. Chanvillard, P. Casaova, G. Orange, No Title, in: 1st FIB Congr. Struct. 21st Century, Osaka, 2002: pp. 105–122.

[52] A. De Chefdebien, F. Robert, C. Colligon, Performance of ultra high strength concrete subjected to fire, in: CONSEC 07 Concr. under Sev. Cond. Environ. Load., Chelles, 2007.

[53] A. Meda, P.G. Gambarova, M. Bonomi, High-performance concrete in fire-exposed reinforced concrete sections, Struct. Eng. 99 (2002) 277–287.

[54] M. Husem, The effects of high temperature on compressive and flexural strengths of ordinary and high-performance concrete, Fire Saf. J. 41 (2006) 155–163. https://doi.org/10.1016/j.firesaf.2005.12.002.

[55] P. Bamonte, P.G. Gambarova, Thermal and Mechanical Properties at High

Temperature of a Very High-Strength Durable Concrete, J. Mater. Civ. Eng. 22 (2010) 545–555. https://doi.org/10.1061/(ASCE)MT.1943-5533.0000058.

[56] T. Ranawaka, M. Mahendran, Experimental study of the mechanical properties of light gauge cold-formed steels at elevated temperatures, Fire Saf. J. 44 (2009) 219–229. https://doi.org/10.1016/j.firesaf.2008.06.006.

[57] C.S. Poon, Z.H. Shui, L. Lam, Compressive behavior of fiber reinforced high-performance concrete subjected to elevated temperatures, Cem. Concr. Res. 34 (2004) 2215–2222. https://doi.org/10.1016/j.cemconres.2004.02.011.

[58] S.P. Chiew, M.S. Zhao, C.K. Lee, Mechanical properties of heat-treated high strength steel under fire/post-fire conditions, J. Constr. Steel Res. 98 (2014) 12–19. https://doi.org/10.1016/j.jcsr.2014.02.003.

[59] X. Qiang, X. Jiang, F.S.K. Bijlaard, H. Kolstein, Mechanical properties and design recommendations of very high strength steel S960 in fire, Eng. Struct. 112 (2016) 60–70. https://doi.org/10.1016/j.engstruct.2016.01.008.

[60] J. Lange, N. Wohlfeil, Examination of the mechanical properties of the microalloyed grain refined steel S 460 at elevated temperatures, Bautechnik. 84 (2007) 711–720.

[61] C. Maraveas, Z.C. Fasoulakis, K.D. Tsavdaridis, Mechanical properties of High and Very High Steel at elevated temperatures and after cooling down, Fire Sci. Rev. 6 (2017). https://doi.org/10.1186/s40038-017-0017-6.

[62] A. Heidarpour, N.S. Tofts, A.H. Korayem, X.-L. Zhao, C.R. Hutchinson, Mechanical properties of very high strength steel at elevated temperatures, Fire Saf. J. 64 (2014) 27–35. https://doi.org/10.1016/j.firesaf.2014.01.006.

[63] L.T. Phan, N.J. Carino, Review of Mechanical Properties of HSC at Elevated Temperature, J. Mater. Civ. Eng. 10 (1998) 58–65. https://doi.org/10.1061/(ASCE)0899-1561(1998)10:1(58).

[64] W. Zheng, H. Li, Y. Wang, Compressive stress–strain relationship of steel fiber-reinforced reactive powder concrete after exposure to elevated temperatures, Constr. Build. Mater. 35 (2012) 931–940. https://doi.org/10.1016/j.conbuildmat.2012.05.031.

[65] B. Persson, Fire resistance of self-compacting concrete, SCC, Mater. Struct. 37 (2004) 575–584. https://doi.org/10.1007/BF02483286.

[66] Y.B. Heva, Behaviour and design of cold-formed steel compression members at elevated temperatures, Queensland University of Technology, 2009.

[67] P. Mäkeläinen, J. Outinen, J. Kesti, Fire design model for structural steel S420M based upon transient-state tensile test results, J. Constr. Steel Res. 48 (1998) 47–

57. https://doi.org/10.1016/S0143-974X(98)00005-4.

[68] J. Chen, B. Young, Experimental investigation of cold-formed steel material at elevated temperatures, Thin-Walled Struct. 45 (2007) 96–110. https://doi.org/10.1016/j.tws.2006.11.003.

[69] K.D. Hertz, Limits of spalling of fire-exposed concrete, Fire Saf. J. 38 (2003) 103–116. https://doi.org/10.1016/S0379-7112(02)00051-6.

[70] M. Bastami, F. Aslani, M. Omran, High-temperature mechanical properties of concrete, Int. J. Civ. Eng. 8 (2010) 337–351.

[71] A. Savva, P. Manita, K.K. Sideris, Influence of elevated temperatures on the mechanical properties of blended cement concretes prepared with limestone and siliceous aggregates, Cem. Concr. Compos. 27 (2005) 239–248. https://doi.org/10.1016/j.cemconcomp.2004.02.013.

[72] A. Buchanan, A. Abu, Structural design for fire safety, 2017.

[73] V. Kodur, M. Naser, Structural Fire Engineering, 1st ed., McGraw Hill Professional, 2020.

[74] H.D. Craveiro, J.P.C. Rodrigues, A. Santiago, L. Laím, Review of the high temperature mechanical and thermal properties of the steels used in cold formed steel structures - The case of the S280 Gd+Z steel, Thin-Walled Struct. 98 (2016) 154–168. https://doi.org/10.1016/j.tws.2015.06.002.

[75] V. Kodur, Properties of Concrete at Elevated Temperatures, ISRN Civ. Eng. 2014 (2014) 1–15. https://doi.org/10.1155/2014/468510.

[76] Q. Ma, R. Guo, Z. Zhao, Z. Lin, K. He, Mechanical properties of concrete at high temperature-A review, Constr. Build. Mater. 93 (2015) 371–383. https://doi.org/10.1016/j.conbuildmat.2015.05.131.

[77] C. Maraveas, Z.C. Fasoulakis, K.D. Tsavdaridis, Mechanical properties of High and Very High Steel at elevated temperatures and after cooling down, Fire Sci. Rev. 6 (2017) 3. https://doi.org/10.1186/s40038-017-0017-6.

[78] P. Stoica, Y. Selen, Model-order selection, IEEE Signal Process. Mag. 21 (2004) 36–47. https://doi.org/10.1109/MSP.2004.1311138.

[79] E.J. Wagenmakers, S. Farrell, AIC model selection using Akaike weights, Psychon. Bull. Rev. 11 (2004) 192–196. https://doi.org/10.3758/BF03206482.

[80] JCSS, JCSS Probabilistic Model Code: Section 3.01, Zurich, Switzerland, 2002.

[81] D. Naus, A compilation of elevated temperature concrete material property data and information for use in assessments of nuclear power plant reinforced concrete structures, 2010.

[82] JCSS, JCSS Probabilistic Model Code: Section 3.02, Zurich, Switzerland, 2001.